International Journal of Heat and Mass Transfer 52 (2009) 1954–1964

Contents lists available at ScienceDirect

International Journal of Heat and Mass Transfer

journal homepage: www.elsevier.com/locate/ijhmt

A hybrid optimization technique for developing heat transfer correlations based on transient experiments

G. Venugopal, Suryakant, C. Balaji *, S.P. Venkateshan

Heat Transfer and Thermal Power Laboratory, Department of Mechanical Engineering, Indian Institute of Technology Madras, Chennai 600 036, India

ARTICLE INFO

Article history:
Received 25 February 2008
Received in revised form 3 July 2008
Available online 16 December 2008

Keywords:
Vertical channel
Transient experiments
Nusselt number
Hybrid optimization
Genetic algorithm
Levenberg–Marquardt algorithm
Simulated annealing

ABSTRACT

A new approach for developing a Nusselt number correlation, in terms of relevant non-dimensional parameters, for turbulent forced convection flows in vertical channels using a judicious combination of transient cooling experiments with a hybrid optimization technique is reported. The temperature–time history, during the cooling of a heated plate, idealized as a lumped capacity heat transfer model, is recorded using a PC based data acquisition system. A numerically computed temperature–time history of the plate is then compared with the experimentally known temperature–time history to estimate the residual. The minimization of sum of the squares of the residual is done using a hybrid numerical optimization technique, i.e. a combination of Genetic Algorithm and the Levenberg–Marquardt method, in order to obtain the coefficient and the exponents of the pertinent non-dimensional parameters in the Nusselt number correlation. The parameters in the correlation are also retrieved using another global optimization technique, the Simulated Annealing (SA), for evaluating the consistency in parameter estimation. As a validation exercise, Nusselt number values estimated using the proposed correlation are compared with steady state experimental results and a good agreement of results endorses the efficacy of this approach.

1. Introduction

Convective heat transfer from surfaces in vertical wall bounded flows occurs in numerous practical engineering applications such as cooling of electronic equipment, nuclear fuel assembly, solar heating systems, plate heat exchangers and so on. It is well known that heat transfer in channel confined flows is greatly influenced by two modes of induced fluid motion. Starting from the very early study of Elenbaas [1], heat transfer due to naturally induced fluid motion caused by density gradients imparted by a temperature difference between the wall surface and the ambient fluid has been extensively investigated in literature. Heat transfer studies on channel confined flows under low and moderate fluid velocity regimes; known as mixed convection heat transfer, has become an important subject of research because this regime entails the simultaneous presence of buoyancy, inertia and viscous forces. In mixed convection heat transfer, the buoyancy forces, externally applied pressure forces and the viscous forces compete with each other thereby affecting the flow dynamics within the system, which in turn influences the heat transfer characteristics too (see Gebhart et al. [2] for a fuller discussion on buoyancy induced flows). A review of literature of heat transfer studies on vertical channel flows indicates that most of the studies are focused on laminar mixed convection and scarce are the studies that report on fully developed turbulent mixed convection. An early study on combined forced and free convective heat transfer in vertical channel is due to Tao [3], which presented an analytical solution for fully developed laminar flow in a vertical channel for the case of constant axial wall temperature gradient with and without heat generation. Agarwal [4] also obtained an analytical solution by a variational method for laminar combined forced and free convection in vertical rectangular channels and circular ducts. Quintiere and Mueller [5] developed an approximate method of analysis, based on a linearization of the governing equations, for developing mixed convection flow between two isothermal vertical surfaces. Yao [6] presented an analytical solution for fluid flow and heat transfer in the entry region of a heated vertical channel for both constant wall temperature and constant wall heat flux conditions and proposed a criterion for natural convection dominance. Numerical studies for predicting developing mixed convection and flow reversal in a vertical channel with asymmetric wall temperatures have been reported by Aung and Worku [7]. Later, the same authors [8] performed studies on combined free and forced convection for buoyancy aiding flow in a vertical parallel plate channel for the case of asymmetric wall heating and uniform heat

* Corresponding author.
E-mail addresses: balaji@iitm.ac.in (C. Balaji), spv@iitm.ac.in (S.P. Venkateshan).

0017-9310/$ - see front matter © 2008 Elsevier Ltd. All rights reserved.
doi:10.1016/j.ijheatmasstransfer.2008.07.054

Nomenclature

A_e	surface area of the main plate not exposed to the side plates, m^2
AR	aspect ratio (D/L)
A_s	surface area of the main plate exposed to the side plates, m^2
A_t	total surface area of the main plate, m^2
Bi	Biot number, hL_c/k_s
Cp	specific heat capacity of the material of main plate, J/kg K
D	depth of the channel, m
F_{ij}	view factor from i^{th} to j^{th} surface
Gr_D	Grashof number, $g\beta(T_h - T_\infty)D^3/\nu^2$
h	heat transfer coefficient, W/m^2 K
J	radiosity, W/m^2
k_f	thermal conductivity of fluid, (air) W/m K
k_s	thermal conductivity of solid(main plate) W/m K
L	height of the main plate, m
L_c	characteristic length for defining the Biot number, m
m	mass of the test plate assembly, kg
$\overline{Nu}_D$	average convective Nusselt number
Pr	Prandtl number of fluid (air)
Q_c	convective heat transfer, W
Q_l	minor heat losses from the heated main plate, W
Q_r	total radiative heat transfer, W
Q_{r1}	radiative heat transfer from the surface of main plate not exposed to side plates, W
Q_{r2}	radiative heat transfer from the surface of main plate exposed to side plates, W
Q_t	total heat transfer, W
Re_D	Reynolds number, DU/ν
Ri_D	Richardson number, Gr_D/Re_D^2
T	temperature, K
t	time, s
U	fluid velocity, m/s

Greek symbols

β	isobaric cubic expansivity of the fluid, K^{-1}
ε	total hemispherical emissivity
σ	Stefan Boltzmann constant, 5.67×10^{-8} W/m^2 K^4
ν	kinematic viscosity of air, m^2/s

Superscripts

exp	experimental
num	numerical

Subscripts

i	initial
h	hot main plate
c	cold side plate
∞	ambient

flux conditions. Closed form solutions were reported by Hamadah and Writz [9] for fully developed laminar mixed convection for buoyancy opposed flow in a vertical channel for different boundary conditions. The authors have presented the velocity profiles and also the criteria for the onset of flow reversal. Watson et al. [10] carried out a numerical investigation of steady laminar mixed convection with conduction in a series of vertical parallel plates with planar heat sources for the cases of buoyancy aided flow. Gururaja Rao et al. [11] performed numerical investigations on mixed convection and surface radiation in vertical channels for both symmetric and asymmetric isothermal walls and proposed correlations for the average convective and radiative Nusselt number for each wall.

A few studies have been reported on fully developed turbulent transport processes of heat and momentum in vertical parallel plate channels. Nakajima et al. [12] investigated, experimentally and numerically, turbulent transport at low Reynolds number flows in a vertical parallel plate channel whose wall temperatures are held constant but can take on different values. Their study highlighted the effect of buoyancy on the turbulent transport process. Chen et al. [13] carried out a finite element analysis of fully developed turbulent flow between vertical parallel plates at different wall temperatures. The numerical simulations were done with a one-equation turbulence model for low Reynolds number flows.

The preceding review of literature reveals that most of the studies on vertical channel confined flows consider either laminar mixed convection or fully developed turbulent mixed convection and the studies are more often theoretical/numerical rather than experimental. However, in many practical situations, the channel walls are of finite length with an opening at each end and are sufficiently wide apart, and therefore evidently the heat transfer characteristics are entirely different from those characterized by fully developed profiles. Furthermore, the correlating equations reported in the above studies for estimating the heat transfer rates from vertically oriented parallel plates are the outcome of steady state analysis only. This work introduces a new approach for developing Nusselt number correlation for low Reynolds number turbulent flows in isolated vertical parallel plate channels, based on transient experimental techniques combined with a hybrid numerical optimization for parameter estimation. The philosophy of applying the transient method to develop a heat transfer correlation is that during the initial stages of cooling of the plate, the instantaneous values of the Grashof number will be higher when compared to those at later stages of the cooling and consequently a wide range of instantaneous Richardson numbers can be obtained in a single experiment, provided a suitable inlet velocity is used for the experiments.

2. Experimental apparatus

The experiments are conducted in an open circuit vertical wind tunnel that can supply a uniform air flow inside the test section. The vertical channel essentially consists of a heated vertical plate (here after referred to as main plate) arranged centrally between two adiabatic side plates. The main plate is made of an assembly of two aluminum plates of dimensions $150 \times 250 \times 3$ mm with a flat heater sandwiched between them. The details of the main plate and the arrangement used to suspend it vertically are reported in an earlier work of the same authors [14]. However, it needs to be mentioned that the earlier study considered laminar, mixed convection from a single vertical plate as opposed to turbulent mixed convection from a vertical channel that is being considered in this study. The vibration of the main plate that would occur at higher air velocities is prevented by using a tie-rod arrangement provided at the two side edges of the main plate. The tie-rod arrangement on each side edge consists of a 35 mm long, 10 mm wide and 0.5 mm thickness pressed sheet steel strip attached to the main plate,

while the other end of the steel strip is connected to a threaded Teflon rod (6 mm Φ). The nuts arranged on the free end of the Teflon rods are tightened to obtain rigidity, thereby overcoming the expected vibration induced by the fluid motion. The tie-rod arrangement is made at a distance of 10 mm above the bottom/leading edge of the main plate. Ten "K-type" (36AWG) stainless steel sheathed thermocouples, five on each aluminum plate, are used for the measurement of temperatures at several locations of the heated plate. They are fixed to the plates using copper cement that has a high thermal conductivity. All thermocouples are calibrated before fixing them into the grooves machined in the plates and the measurement error is within ±0.2 °C.

Aluminum plates of 3 mm thickness are used for making the side plates. The side plates attached to wooden boxes are made from 6 mm plywood panel and these plates are thermally insulated from their back side using non-rubberised cork sheet (25 mm thickness) and Thermocole® balls. The wooden boxes carrying the side plates are arranged symmetrically on either side of the main plate and are fixed to the test section by employing L shaped mild steel brackets. The groove made in the L brackets provides flexibility in mounting the boxes at the desired position thus ensuring the dimensional accuracy of the channel. K-type thermocouples are used to record the temperatures at several locations on the side plates. All thermocouples are connected to a PC based Data acquisition system (Model No.34970A, Agilent Technologies Ltd.), through compensating wires. The power input to the heater is supplied from a regulated DC power source which has a range of 30–600 V and 0–1.5 A. The main plate can be heated to different temperature levels by controlling the power input to the heater. The power input to the heater is calculated by measuring the voltage and current using two digital multimeters. A buffing operation is done for obtaining polished surface for all plates. The surface roughness of the buffed plate is measured using a surface texture measuring instrument (PERTHOMETER) and the surface roughness (Ra) is estimated as 0.083 μm. The velocity and temperature of the air inside the test section are measured using a thermal anemometer (AIRFLOW™ TA5) and the velocity measurement is done at a location 4 cm below the leading edge of the heated plate. Using an arrangement for traversing the anemometer, the velocity measurement is done at four different locations upstream of the main plate. The mean value of the velocities is used for calculating the Reynolds number. The air velocity is varied by varying the speed of the axial flow fan mounted appropriately below the diffuser entry. To avoid vibrations getting induced in the tunnel during the operation of the fan, the fan is independently supported on a metallic frame with its exit slightly below the diffuser entry. The thermophysical properties for air, which is at atmospheric pressure, are estimated at the film temperature, T_f. A bell mouth entry ensures that the flow of air entering the channel is uniform. The details of experimental set up are depicted in Fig. 1.

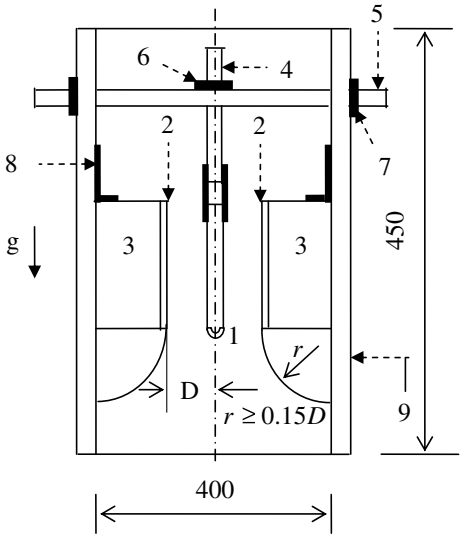

Fig. 1. Schematic diagram of the experimental set up for the study of forced convection in vertical parallel plate channels [shown here are the arrangement in the test section (400 × 450 × 530 mm) of the wind tunnel]. 1. Main plate (150 × 250 × 6 mm). 2. Side plates (150 × 250 × 3 mm) 3. Wooden boxes. 4. Teflon rod. 5. Stainless steel rod. 6. Adjusting nut. 7. Adjusting nut. 8. L brackets. 9. Wooden side walls.

3. Transient experimental technique for developing the correlation

The principal objective of this study is concerned with the retrieval of the parameters (a, b and c) in the Nusselt number correlation of a form, $\overline{Nu}_D = a(1 + Ri_D)^b Re_D^c$, for low Reynolds number turbulent flows in vertical parallel plate channels using transient experimental techniques combined with a hybrid numerical optimization. In doing the transient cooling experiments, the heated plate is treated as a lumped capacity heat transfer model. It is well known that the established criterion for defining a heat transfer model as a lumped capacity system is the Biot number. In this study, the average convective heat transfer coefficient is estimated as 19.72 W/m^{2}K (corresponding to a maximum value of convective Nusselt number, Nu_{cD} = 35.45, estimated) and if the contribution due to radiation heat transfer is roughly estimated as 20% of the convective heat transfer coefficient, then the overall heat transfer coefficient is estimated to be 23.66 W/m^2 K. Using this value of the overall heat transfer coefficient, for a characteristic length 2.82 mm and a thermal conductivity of 240 W/m K of the plate material, the Biot number calculated for this transient problem turns out to be 2.78×10^{-4} and hence the validity of lumped capacity formulation is justified.

3.1. Experimental procedure

Initially, the main plate is heated by supplying a known amount of electrical power and the power is switched off after steady state conditions are reached. The transient response of the system is recorded using the data acquisition system and this is done at regular intervals of 30 s till the plate reaches a temperature 5 °C above the ambient temperature. The thermocouple that indicates the temperature close to the average temperature of the plate is chosen for recording the transient response of the system. The experiments are repeated for several initial temperatures of the main plate and different velocities upstream of the main plate. The velocity of air at the inlet of the channel is so chosen that the flow through the channels is turbulent. The velocity values chosen for ensuring turbulent flows are evaluated based on the fact [15] that laminar flow between stationary parallel plates becomes turbulent for Reynolds numbers (defined as $Re = \rho VD/\mu$) greater than approximately 1400. The transition to turbulence has also been independently confirmed in the steady state experiments conducted as a part of this study and is discussed in Section 4.2.2. The experiments were performed in a channel with a spacing of D = 0.051 m. A maximum spatial variation of ±2 °C among the readings of the ten thermocouples is a fair indication of the near isothermal nature of the heated main plate.

3.2. Mathematical formulation

The mathematical model of transient cooling of a heat transfer model which is idealized as a lumped system is given by

$$-mc_p\frac{dT_h}{dt}=\varepsilon\sigma F_{12}A_s(T_h^4-T_c^4)+\varepsilon\sigma F_{13}A_s(T_h^4-T_\infty^4)+\varepsilon\sigma A_e(T_h^4-T_\infty^4)+hA_t(T_h-T_\infty)+Q_l \quad (1)$$

The term on the left hand side represents the rate of change of enthalpy of the plate at time, t. The radiative and convective heat losses, respectively, are represented by the first three terms and the fourth term on the right hand side of Eq. (1). The term Q_l stands for a correction term to account for the unaccountable heat losses. In this study, it is assumed that such losses can be neglected compared to the heat flow normal to the surface. The convective heat transfer coefficient is replaced with the Nusselt number correlation, assumed to be of the form, $\overline{Nu}_D=a(1+Ri_D)^bRe_D^c$ as mentioned earlier. Since the constants appearing in the Nusselt number correlation are to be determined from these transient experiments, Eq. (1) is modified to take the form,

$$-mc_p\frac{dT_h}{dt}=\varepsilon\sigma F_{12}A_s(T_h^4-T_c^4)+\varepsilon\sigma F_{13}A_s(T_h^4-T_\infty^4)+\varepsilon\sigma A_e(T_h^4-T_\infty^4)+[a(1+Ri_D)^bRe_D^c]\frac{k_f}{D}A_t(T_h-T_\infty) \quad (2)$$

The key point in the transient technique employed in the study is the assumption that the thermal equilibration of the plate, as it loses the heat, is almost instantaneous. Such an assumption is truly valid for plate materials of high thermal conductivity that are at the same time not very thick. Moreover, it is clear that the heat release during the transient cooling is also controlled by the two thermophysical properties, specific heat and emissivity, and hence the temperature dependency of these properties should be taken into account for the accurate computation of the transient response of the plate. The variation of specific heat and emissivity with temperature was determined by a method proposed by the authors in an earlier study [16] and thus the temperature dependency of the thermophysical properties encountered in the problem is adequately addressed. The mass of the test plate assembly, inclusive of the mass of heater, was measured using an electronic balance having resolution of 0.001 kg and the value was determined to be 0.698 kg. The view factor between the hot and cold walls is evaluated using an analytical expression [17] for two parallel rectangles of equal size that faces each other.

Eq. (2) is a first order ordinary differential equation, the solution of which for a given initial condition, known ambient temperature and known or assumed values of system parameters (a, b, c, ε, D, F_{12}, F_{13}, A_s, m, c_p) gives the transient response of the plate. The computation of transient response of the system by solving the model Eq. (2) is known as the forward model. In the problem considered here, the interest is to retrieve the parameters in the Nusselt number correlation from the measured transient response of the system, by using a parameter estimation algorithm. Basically, parameter estimation from the experimentally known transient response of the system is an inverse problem and the optimum values of the parameters are estimated by treating the problem as an optimization problem, requiring the minimization of the square of the residuals between the experimental and simulated temperatures using guess values of the parameters.

3.3. Solution procedure

3.3.1. Forward problem

Eq. (2) can be written as

$$\frac{dT_h^{num}}{dt}=\psi(X) \quad (3)$$

where X is the unknown vector defined as, $X=\{a,\ b,\ c\}^T$. Eq. (3) known as the forward problem is an initial value problem, and is solved by a sixth order Runge–Kutta method to obtain the transient response, subject to the initial condition $T_h=T_i$ at $t=0$ and with initial guess values for all the parameters to be retrieved.

3.3.2. Inverse problem

The inverse problem considered here is concerned with the estimation of parameters encountered in the Nusselt number correlation, $\overline{Nu}_D=a(1+Ri_D)^bRe_D^c$ from a knowledge of the measured temperatures. The formulation of the inverse problem is similar to that of the forward problem, except that the parameters, a, b and c are unknown. Instead, measured temperatures of the plate (T_h^{exp}), are available. The inverse problem consists then of utilizing the measured data (T_h^{exp}) to determine the three elements of the unknown vector X defined as

$$R(X)=\sum_{i=1}^{N_{data}}\left[T_h^{exp}-T_h^{num}(X)\right]^2 \quad (4)$$

where T_h^{num} is the simulated data. All of the arguments of $X=\{a,\ b,\ c\}^T$ will be referred to as parameters. The optimization problem is then concerned with the minimization of norm 'R', with respect to each element of the unknown vector 'X'. In this study, a hybrid numerical optimization technique that combines the Genetic Algorithm (GA) with the Levenberg–Marquardt algorithm (LMA) is used for the retrieval of parameters by minimizing the norm 'R'.

3.4. Solution of Inverse problem by hybridization of GA with LMA

In parameter estimation, optimization is invariably used to minimize the errors between measured and estimated data (Eq. (4)). Numerical procedures based on gradient (deterministic) and stochastic methods are two basic types of optimization algorithms commonly employed in practice. The former is known to be a local inversion algorithm and the latter a global inversion algorithm. Among the popular local inversion algorithms are the steepest decent, Newton algorithm, conjugate gradient algorithm, Levenberg–Marquardt algorithm and so on. On the other hand, stochastic based inversion algorithms work on a global search technique to determine approximate solutions for optimization problems. Some examples of this class of algorithms are Genetic Algorithms (GAs), Simulated Annealing (SA), Response Surface Methodology (RSM) and so on. Each local and global optimization algorithm has its own specific features. As the gradient based methods use the information about the behavior of a function by searching along the gradient direction, they are usually faster in their convergence and ensure high level of accuracy in the estimated values at the optimum point. In this way, deterministic techniques are attractive from a computational point of view. However, when local type inversion algorithms are adopted, accurate and reliable results can be obtained only if the starting trial solution is close enough to the actual solutions. Convergence of global optimization techniques in general is not dependent on the guess values. However, stochastic methods generally present a low convergence rate and require a large number of cost function evaluations to achieve a satisfactory convergence threshold. Consequently, they are computationally expensive especially when compared to deterministic optimization techniques. An effective way of improving the convergence rate and reducing the computational time ***simultaneously*** is the hybridization of stochastic methods with deterministic technique, aiming at fully utilizing the complementary advantages of deterministic and stochastic techniques. The simplest way to implement a hybridized version of a stochastic method is that of considering a two stage optimization [18]. In such a hybrid approach, the stochastic method is run for a small number of generations or iterations, requiring therefore a much smaller number of function evaluations. The solution obtained with the stochastic method is then used as the initial guess for

the gradient based methods. In this work, the hybridization of a Genetic Algorithm (GA) with Levenberg–Marquardt algorithm is implemented to estimate the optimum values of the parameters pertinent to the problem considered here. Initially, a GA is used to perform a preliminary search in the solution space and to locate the neighborhood of the solution. Then, using the best solution found with the GA as the initial guess, the Levenberg–Marquardt method is implemented to refine, improve the current solution and quickly converge towards the optimum.

3.4.1. Genetic algorithms

Genetic Algorithms (GAs) are procedures based on mechanics of natural selection and genetics, developed by Holland [19]. GAs emulate genetic recombination and evolution in nature to solve optimization problems. They operate on a randomly generated population in the search space simultaneously and perform a global optimization by the three genetic operations, i.e. selection, cross over and mutation. According to the evolutionary theory, only the most suited elements of a population can survive and generate offsprings, thereby transmitting their biological heredity to new generations. The suitability of each element according to the problem under consideration is evaluated via a fitness value, directly derived from the objective function. The evolution mechanisms are constituted by the three specific genetic operations mentioned earlier. The cycle of evolution is generally repeated until a predefined number of generations is reached. The GAs are less prone to converge to a local optimum than the gradient based algorithms, even when the initial guess is far away from the exact one because they are stochastic and global in nature. Detailed discussions of GAs can be seen in several references (see for example [20–22]). Since the traditional GA works with only maximization problems, for the optimization problem considered in this study, the objective function is modified as

$$F = \frac{1}{(1+R)} \tag{5}$$

In executing the GA, the following values of input parameters are used.

Population size = 12 ($4n$, where 'n' is the number of parameters to be estimated).

Total string length = 60 (20 for each design variable).

Probability of crossover = 0.5.

Probability of mutation = 0.02.

3.4.2. Levenberg–Marquardt algorithm

The Levenberg–Marquardt algorithm provides a numerical solution to the mathematical problem of minimizing a sum of squares of several, generally, nonlinear functions that depend on a common set of parameters. The least square problem, in this study, consists of finding the parameter vector $X = \{a,\ b,\ c\}^T$ for which the objective function $R(X) = f^T f = \Sigma_{i=1}^{N_{data}} [T_h^{\exp} - T_h^{\mathrm{num}}(X)]^2$ becomes minimum, where $f(X)$ is the difference between the measured and simulated values. The parameters which minimize the objective function $R(X)$ satisfy a set of nonlinear algebraic equations which are obtained by differentiating Eq. (4) with respect to each element of the unknown vector 'X' and setting these derivatives equal to zero. The resulting system of algebraic equations represented by $(J^T J)\Delta X = -J^T f$, where J is the Jacobian of f at X, is then solved by Levenberg–Marquardt iterative procedure. In order to improve the convergence of the solution of the resulting system of equations a non-negative damping parameter λ is added to yield the Levenberg–Marquardt algorithm [23].

$$(J^T J + \lambda I)\Delta X = -J^T f \tag{6}$$

In the Levenberg–Marquardt algorithm, by setting a large value of damping parameter, the steepest descent method is initially followed. Thereafter, with the use of a small value of damping parameter, Newton's method is adopted. The Levenberg–Marquardt algorithm, like other numerical minimization algorithms, is an iterative procedure that starts with an initial guess for the vector of unknowns, X^o. In each iteration step, the parameter vector X, is replaced with X^{k+1}, defined as $X^{k+1} = X^k + \Delta X^k$. The incremental value of unknown parameters ΔX, is obtained from Eq. (6). Writing Eq. (6) in a more general form suitable for iterative calculations

$$\Delta X^k = -\left[(J^k)^T J^k + \lambda^k I\right]^{-1} (J^k)^T f^k \tag{7}$$

gives the new estimated values for the unknown parameters, $X^{k+1} = X^k + \Delta X^k$. For a fuller discussion on the algorithm, see [21,24].

4. Results and discussion

Fig. 2 shows the route map for solving the parameter retrieval problem considered in this study. In using the GA, the initial population is randomly generated in the search space assigned for the design variables. The search space for the design variables, for this problem, is; $0.01 \leqslant a \leqslant 0.08$, $1 \leqslant b \leqslant 10$ and $0.3 \leqslant c \leqslant 0.85$. In fact, the bounds are *a priori* chosen for each design variable based on earlier studies conducted on parallel plate channels reported in literature. An in-house code is developed for LMA and the GA code originally developed by Carroll [25] is modified for solving the inverse heat transfer model. The programs are executed on a Pentium 4 machine with a 3 GHz processor and 2 GB RAM. Temperature data from five transient cooling experiments with different initial temperatures were used for the parameter estimation. The experiments were conducted on a channel with aspect ratio, $AR = 0.341$. The temperature dependency of specific heat capacity of the plate material and emissivity are estimated as $741.59 + 0.478T$ and $0.048 + 4.27 \times 10^{-6}T$, respectively [16].

It is noted that when lower bounds of the parameters are used as the initial guess values for executing the LMA, the parameters are estimated as; $a = 0.02341$, $b = 1.0$ and $c = 0.85$. On the other hand, when upper bounds of the parameters are used as the initial guess values the solution yields $a = 0.01684$, $b = 10$ and $c = 0.85$. This shows that in probing global optima for multimodal problems using gradient based methods with arbitrary chosen guess values from a large search space of the design variables, the solution may get trapped into a local extreme or even diverge. The foregoing analysis, therefore, establishes the need for hybridization of optimization techniques for the problem under consideration. Table 1 indicates the values of parameters retrieved using GA from five transient experiments, together with the time taken for carrying out a certain number of generations (iterations so to speak). As can be seen from the Table, no appreciable change is observed between the values of parameters retrieved after 300 and 400 generations and therefore it can be inferred that after 300 generations, the estimated parameters have reached the optimum values. An inherent feature of GAs is that as they mimic mechanics of natural evolution, better and better values will be generated as the generations proceed. However, often times the improvement may not be substantial from a mathematical view point. In view of this, a subsequent implementation of a gradient based method after some iterations with the GA may be appropriate for the refinement of the solution vector. It is seen from Table 1 that the values of the parameters retrieved after 100 generations is close to the global optimum and this is evident from Fig. 3. So it is reasonable to implement Levenberg–Marquardt method, taking initial guess values from GA output after 100 generations, to refine and improve the solution. Table 2 shows the results of parameter estimation

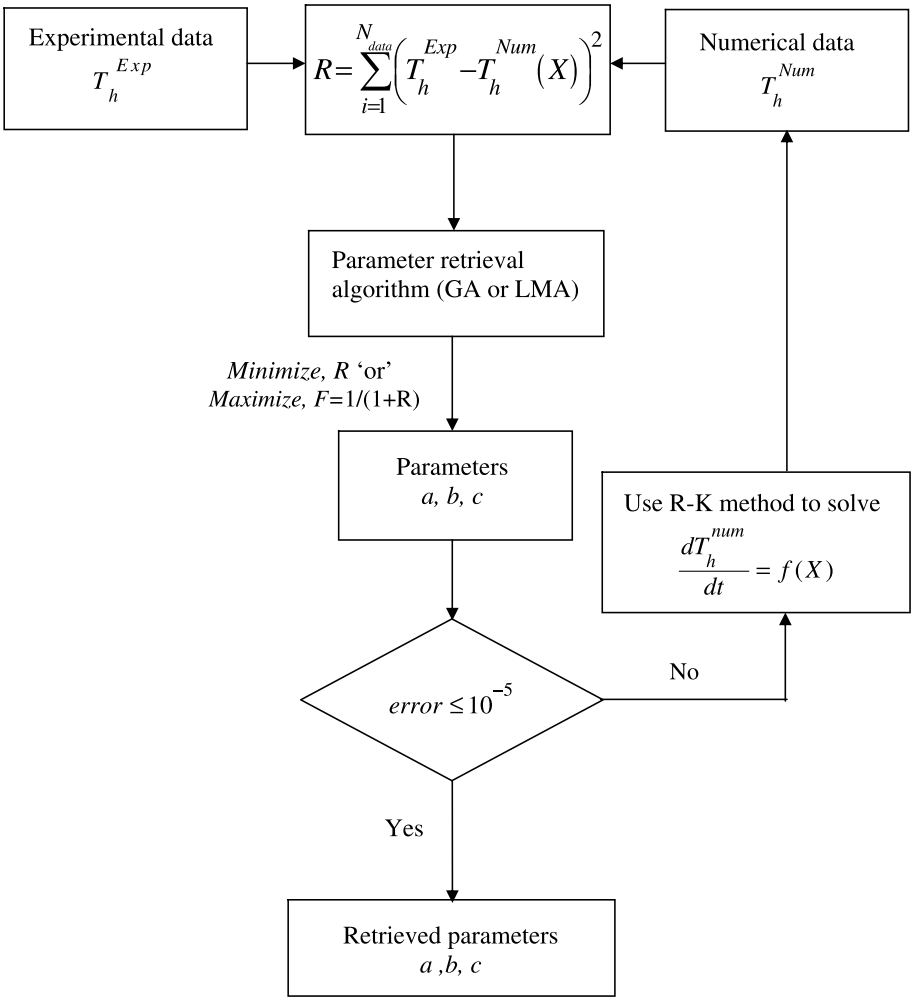

Fig. 2. Route map for solving the parameter retrieval problem.

Table 1
Values of the parameters retrieved using GA.

Case no	Initial temp (K)	No. of generations	Retrieved parameters			CPU time, s
			a	*b*	*c*	
1	405.7	100	0.037681	2.380983	0.785631	90.05
		200	0.037815	2.207287	0.785811	180.63
	$(0.0005 \leqslant Ri_D \leqslant 0.058)$	300	0.037914	2.207149	0.785810	271.55
		400	0.037914	2.207184	0.785810	362.39
2	432.4	100	0.038312	2.161410	0.793529	86.67
		200	0.038430	2.125116	0.793510	172.50
	$(0.012 \leqslant Ri_D \leqslant 0.207)$	300	0.038430	2.125001	0.793510	257.84
3	424.6	100	0.040087	2.335793	0.785679	69.08
		200	0.040087	2.335793	0.785679	137.36
	$(0.002 \leqslant Ri_D \leqslant 0.131)$	300	0.040071	2.373094	0.785656	208.84
4	415.9	100	0.040141	1.936501	0.780217	67.98
		200	0.040137	1.936410	0.780223	134.50
	$(0.0005 \leqslant Ri_D \leqslant 0.09)$	300	0.040151	2.016240	0.780785	203.83
5	433.7	100	0.037736	2.207416	0.786716	61.47
		200	0.037753	2.204926	0.786704	121.92
	$(0.0005 \leqslant Ri_D \leqslant 0.065)$	300	0.037822	2.204922	0.786715	182.17

after 100 generations of GA, LMA implemented after 100 generations of GA and after 300 generations of GA, respectively, for each experiment. The hybrid optimization method yields matching results with those predicted by GA after 300 generations, and more importantly, the convergence is extremely fast thereby saving a considerable amount of computation time. This is more advantageous when a large number of parameters are to be estimated while handling more complex inverse problems. The mean and

standard deviation of the values of the retrieved parameters are estimated and are shown in Table 2. The mean value of the parameters are then used to propose the Nusselt number correlation of the required form which is

$$\overline{Nu}_D = 0.039(1 + Ri_D)^{2.334}\ Re_D^{0.787} \tag{8}$$

for

$$\begin{bmatrix} 0.0005 \leqslant Ri_D \leqslant 0.207 \\ 2000 \leqslant Re_D \leqslant 6000 \end{bmatrix}$$

In order to judge the authenticity of the parameters retrieved using this transient experimental technique, the value of the coefficient and exponent of Reynolds number in Eq. (8) are first compared with those reported in literature [13] for fully developed turbulent flow in vertical channels. The correlation reported in [13] has the form, $Nu_c = 0.021Re^{0.8}\mathrm{Pr}^{0.4}$. A larger value of coefficient in Eq. (8) is admissible because higher heat transfer rates are expected from widely spaced channels of finite length than that are caused by fully developed profiles from narrow channels. Gau et al. [26], observed that in the case of low Reynolds number turbulent flows, especially in the transition regime, the buoyancy parameter can slightly increase the average Nusselt number for buoyancy assisting flow. The small drop in the value of exponent of Reynolds number is attributed to the effect of buoyancy parameter on the heat transfer in aiding convection in the range of parameters applicable to Eq. (8). The standard deviation of the values of the parameters reported in the correlating Eq. (8) are $\varphi_a = \pm 0.001$, $\varphi_b = \pm 0.175$ and $\varphi_c = \pm 0.005$ and the percentage difference with respect to the corresponding mean values of the estimated parameters are ±2.56%, ±7.49% and ±0.64%, respectively. Small values of standard deviations indicate the consistency of the values of the parameters estimated.

4.1. Sensitivity study

Finally, to estimate how far the retrieved parameters are sensitive to the noise in the temperature measurement, the parameters are re-estimated after perturbing the measured temperature by adding random noise. The effect of noise is taken into account artificially as, $T_i^{\text{with error}} = T_i^{\text{meas}} + \phi\ \omega$, where $T_i^{\text{with error}}$ is the corrected temperature, T_i^{meas} is the measured temperature, φ is the standard deviation of the measurement error and ω is a random number. Three cases with random noise level $\varphi = 0.1$, 0.2 and 0.3, were considered. The value of ω is randomly generated and chosen over the range $-2.576 < \omega < 2.576$, which represents the 99% confidence bound for the temperature measurement. Table 3 shows the values of the parameters re-estimated after perturbing the measured temperatures with Gaussian noise for different values of φ. The values reported in the Table are the result of error analysis done for experiment numbers 1 and 5. The results show that for small values of φ, the values of the retrieved parameters are consistent. However, for $\varphi = 0.3$, the numerical values of the estimated parameters indicate that the measurement errors amplify the estimated errors. Moreover, it indicates that the proposed method provides accurate and stable values of the parameters when a realistic error level is used. In general, from the results of the sensitivity study, it can be concluded that an increase in the measurement errors causes a decrease in the accuracy of the inverse solution, as expected.

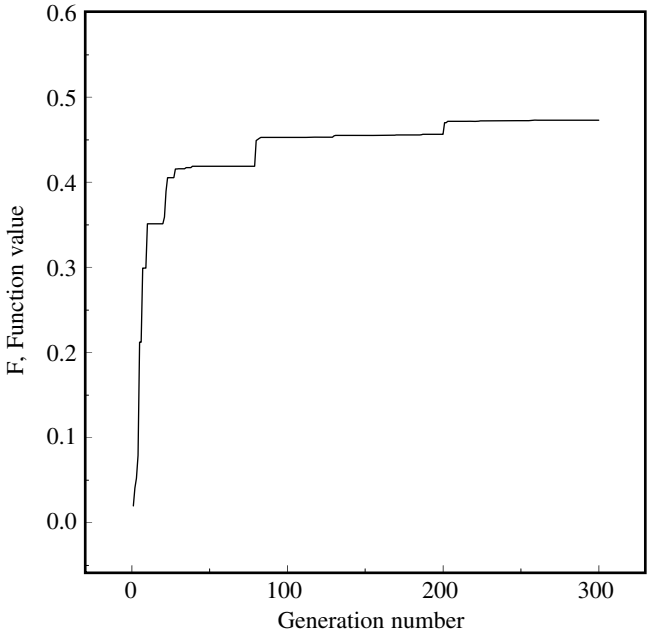

Fig. 3. Variation of function value (F) with generations.

4.2. Validation

4.2.1. Parameter retrieval using simulated annealing (SA)

The consistency in the parameter estimation is further assessed by employing another probabilistic global optimization method called Simulated Annealing for the parameter estimation. Simulated Annealing (SA) as a meta-heuristic method to solve combinatorial problems has been widely accepted for various optimization problems. SA performs really well for nonlinear problems to achieve near optimal results with a computational time constraint. Together with GAs, SA is the first of a few among the various random search methods that have been tested for different benchmark real life problems. Very much like GA, SA works with direct objective function evaluation, thereby avoiding calculation of gradients of functions, thus making it suitable for a wide variety of problems where derivatives are unknown or are difficult or expensive to calculate.

SA mimics the physical process by which a material changes state with decrease in its temperature relative to its energy level. A heated material is in a higher energy state of random configuration which gets organized with slow cooling. It reaches a crystalline or an organized state, which is more ordered with a lower energy state configuration. Simulating the same physical process for solving a combinatorial problem, SA starts with a random solution representing a higher energy state of a material. Slowly, the temperature is brought down and solution reaches optimum energy state satisfying various constraints. As a global optimization technique, there is a need to avoid local minima while descending down the energy hill. This is taken care by using the powerful Metropolis algorithm and retaining some of the rejected solutions based on a stochastic accept/reject criterion. The numbers of rejected solutions retained vary at different temperature. At higher temperatures, the condition for retaining a rejected solution is less stringent in order to allow search in a larger domain. As the temperature comes down, the Metropolis condition is made stringent in order to get a better convergence. More details of the algorithm are available in Deb [27].

Simulated Annealing is a point to point search method. Here, instead, a population based approach for thorough search of domain has been incorporated. The population based approach is an improvement over point based approach where like GA simultaneously several candidates are tested for their fitness. As can be seen with different new age evolutionary algorithms like ant colony optimization, particle swarm optimization and so on, population based search techniques search the solution space thoroughly and at the same time avoid premature convergence.

Table 2
Parameters retrieved using GA and hybridization of GA with LMA.

Case no	Initial temp (K)	Algorithm	Retrieved parameters			CPU time, s
			a	*b*	*c*	
1	405.7	GA[a]	0.03768	2.38098	0.78563	90.05
		GA[a] + LMA	0.03780	2.52441	0.78599	93.18
	($0.0005 \leqslant Ri_D \leqslant 0.058$)	GA[b]	0.03791	2.20715	0.78581	271.55
2	432.4	GA[a]	0.03831	2.16141	0.79353	86.67
		GA[a] + LMA	0.03846	2.21466	0.79406	94.92
	($0.012 \leqslant Ri_D \leqslant 0.207$)	GA[b]	0.03843	2.12500	0.79351	257.84
3	424.6	GA[a]	0.04009	2.33579	0.78568	69.08
		GA[a] + LMA	0.04012	2.50814	0.78593	72.85
	($0.002 \leqslant Ri_D \leqslant 0.131$)	GA[b]	0.04007	2.37309	0.78566	208.84
4	415.9	GA[a]	0.04014	1.93650	0.78022	67.98
		GA[a] + LMA	0.04081	2.13580	0.78000	73.03
	($0.0005 \leqslant Ri_D \leqslant 0.09$)	GA[b]	0.04015	2.01624.	0.78079	203.83
5	433.7	GA[a]	0.03774	2.20742	0.78672	61.47
		GA[a] + LMA	0.03790	2.28946	0.78722	65.89
	($0.0005 \leqslant Ri_D \leqslant 0.065$)	GA[b]	0.03782	2.20492	0.78672	182.17
Mean			0.039	2.334	0.787	
Std. deviation			±0.001	±0.175	±0.005	

[a] GA output after 100 generations.
[b] GA output after 300 generations.

Table 3
Values of the retrieved parameters using GA* + LMA for different values of the measurement error (i.e. $\varphi = 0.0$, 0.1, 0.2 and 0.3).

Case no	Initial temp (K)	Std. deviation of error (φ)	Retrieved parameters		
			a	*b*	*c*
1	405.7	0.0	0.03780	2.52441	0.78599
		0.1	0.03760	2.13827	0.78648
		0.2	0.03843	2.16597	0.78336
		0.3	0.04233	2.16263	0.77246
5	433.7	0.0	0.03790	2.28946	0.78722
		0.1	0.03666	1.93206	0.79151
		0.2	0.03895	2.26657	0.78261
		0.3	0.03789	2.34899	0.78577

For the problem under consideration the population size is 20. Among the various candidates of the population the solution with the best fit with experimental data is reported each time the temperature drops. Different solutions thus searching the domain improve the probability and the efficiency of the search process. The input parameters used for SA coding are

Population size = 20.
Initial temperature = 400 K.
Temperature drop per iteration = 1 K.
Number of objective function evaluations in each iteration = 1 for each solution.

Acceptance probability $\leqslant \exp((R' - R)/T)$ (where R') is objective function value of previous solution, R is objective function value of new solution and T is the temperature in Kelvin) and R is same as defined in Eq. (4).

A program developed for executing the Simulated Annealing using a fourth order Runge–Kutta method is used for the numerical solution of the forward model represented by Eq. (3). Fig. 4 shows the convergence history of SA, as the iterations proceed. The results of the SA are shown in Table 4 and are in concordance with the GA results. This can thus be treated as validation for the methodology of the hybridization strategy of using a random search technique for obtaining a near optimal parameter and then utilizing it to achieve an exact solution using the gradient based method that was reported in the earlier section. Fig. 5 shows the estimated error between measured and simulated temperatures for a transient experiment (Expt.No.1) using different optimization methods employed for parameter estimation. The proximity of the experimental and simulated temperatures is an indication that the parameter estimation is robust. A maximum error of 0.47 K that is observed during the initial phase of cooling process may be due to larger uncertainty in heat loss estimation induced by rapid cooling rate. The variance of the error between the measured and simulated temperatures estimated for different optimization methods employed in the study viz. hybridization of GA with LMA, GA after 300 generations and SA, respectively, are obtained as 0.0165, 0.0195 and 0.0419. The result reveals that the hybridization of a stochastic method with a gradient based method provides more accurate result as compared to those given by stochastic methods when they are implemented independently.

4.2.2. Comparison with steady state experimental results

Steady state experimental procedure: A stabilized D C is supplied to the heater to heat the main plate and the system is then allowed to reach steady state conditions. Steady state is assumed to be reached when the temperature of the heated main plate is observed to vary within ±0.1 °C in 10 min. The temperature and velocity measurements are done after the system has reaches steady state conditions. The experiments were repeated for several power inputs to the heater and different velocities upstream of the channel.

The energy balance at steady state gives

$$Q_t = Q_c + Q_r + Q_l \tag{9}$$

The term, Q_l, stands for the minor heat losses from the heated plate which include the conduction heat loss through the thermocouple wires attached to the main plate, conduction heat loss through the Teflon® rods and the heat loss through the steel strips. The heat loss by conduction through the thermocouple wires is estimated using lead wire model approach outlined in [28]. The heat loss through the Teflon rod ($k = 0.23$ W/mK) is estimated using a one dimensional fin model and that from the steel strip is evaluated by modeling it as a plate fin attached to the heated plate. These quantities, respectively, are estimated as 0.31, 0.12 and 3.21%, corresponding to a power input 139.29W. As these

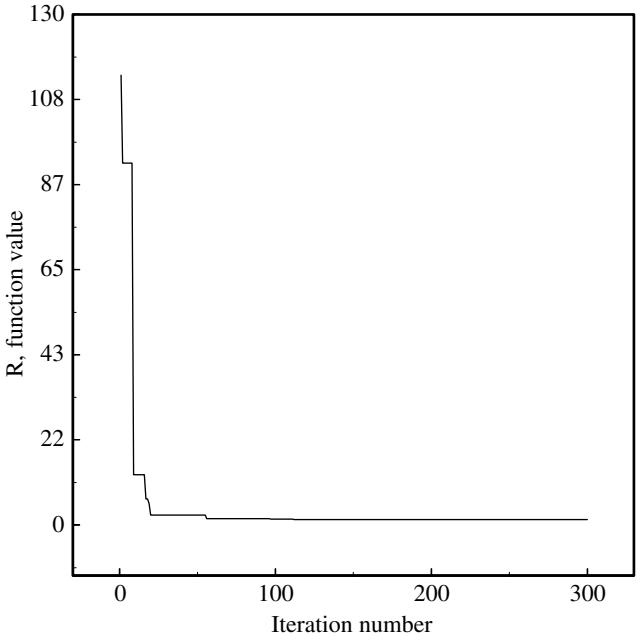

Fig. 4. Convergence history of Simulated Annealing.

quantities are negligible compared to the total heat transfer rate, such losses are neglected. The mean of the temperatures of the main plate and side plates is used for the estimation of radiative (Q_r) and convective heat transfer (Q_c) rates. The radiative heat exchange, Q_r, at the heated plate comprises of two components, viz., the radiative heat exchange at the heated plate that has zero shape factor with the cold plates and that at the heated plate that has non-zero shape factor with the cold plates. The radiative heat exchange at the heated plate that has zero shape factor with the cold plates is calculated using the equation,

$$Q_{r_1} = \varepsilon\sigma A_e(T_h^4 - T_\infty^4) \tag{10}$$

The radiation heat exchange at the hot surface that has non-zero shape factor with the cold plates is computed using the radiosity–irradiation formulation. The non-zero shape factor between the hot and cold walls is evaluated using the analytical expression for two parallel rectangles of equal size that face each other. The radiation heat exchange at the ith surface can be calculated using the formula,

$$Q_i = \frac{\varepsilon_i A_i(\sigma T_i^4 - J_i)}{(1-\varepsilon_i)}, \quad i = 1,2,3, \tag{11}$$

Of the three unknown radiosities, the radiosity of the ambient (J_3) is estimated by treating it as a black body at the ambient temperature. The application of radiosity–irradiation formulation results in two simultaneous equations in two unknowns, the solution of which provides the radiosities J_1 and J_2, and thus enables one to estimate the radiation heat exchange at the lateral face (Q_{r2}) of the heated plate. The total radiation heat exchange at the heated plate is now obtained from

$$Q_r = Q_{r_1} + 2Q_{r_2} \tag{12}$$

The convective heat transfer, Q_c, is then estimated, when the radiation heat exchange is removed from the total heat dissipated, from which the average convective heat transfer coefficient and the convective Nusselt number are computed as follows:

$$h = \frac{Q_c}{A_t \Delta T} \tag{13}$$

$$\overline{Nu}_D = \frac{hD}{k_f} \tag{14}$$

Steady experiments were conducted under a wide range of forced flow conditions during which the Reynolds number varied in the range $700 < Re_D < 12000$. From Fig. 6, it is clearly seen that Nusselt number exhibits different trends at very low and very high Reynolds numbers. The difference in the slopes of the curves, as Reynolds number varies, is a clear indication of rate of thermal energy transport under different flow regimes. Data points at low Reynolds number values less than approximately 2000 exhibit a unique trend whereas those at large values of Reynolds number greater than approximately 6000 have a different unique trend. The observed trend actually justifies the observation made in earlier studies [15] that the flow changes from the laminar regime for Reynolds numbers (defined as $Re = \rho VD/\mu$) greater than approximately 1400. Taking this into consideration, in this study too, a representative transition Reynolds number of $Re_{D,cr} = 1400$ is assumed to delineate the flow regimes into laminar and turbulent.

A comparison of the Nusselt number values estimated using the proposed correlation (Eq. (8)) and those evaluated from steady state data is shown in the form of a parity plot in Fig. 7. The com-

Table 4
Comparison of retrieved values of the parameters using various numerical optimization methods.

Case no	Initial temp(K)	Algorithm	Retrieved parameters		
			a	b	c
1	405.7	GA[a] + LMA	0.03780	2.52441	0.78599
		GA[b]	0.03791	2.20715	0.78581
	$(0.0005 \leqslant Ri_D \leqslant 0.058)$	SA	0.03847	2.39515	0.79466
2	432.4	GA[a] + LMA	0.03846	2.21466	0.79406
		GA[b]	0.03843	2.12500	0.79351
	$(0.012 \leqslant Ri_D \leqslant 0.207)$	SA	0.04059	2.11521	0.78729
3	424.6	GA[a] + LMA	0.04012	2.50814	0.78593
		GA[b]	0.04007	2.37309	0.78566
	$(0.002 \leqslant Ri_D \leqslant 0.131)$	SA	0.04056	2.82382	0.78415
4	415.9	GA[a] + LMA	0.04081	2.13580	0.78000
		GA[b]	0.04015	2.01624	0.78079
	$(0.0005 \leqslant Ri_D \leqslant 0.09)$	SA	0.03816	2.26358	0.80565
5	433.7	GA[a] + LMA	0.03790	2.28946	0.78722
		GA[b]	0.03782	2.20492	0.78672
	$(0.0005 \leqslant Ri_D \leqslant 0.065)$	SA	0.03717	2.58001	0.78856

[a] GA output after 100 generations.
[b] GA output after 300 generations.

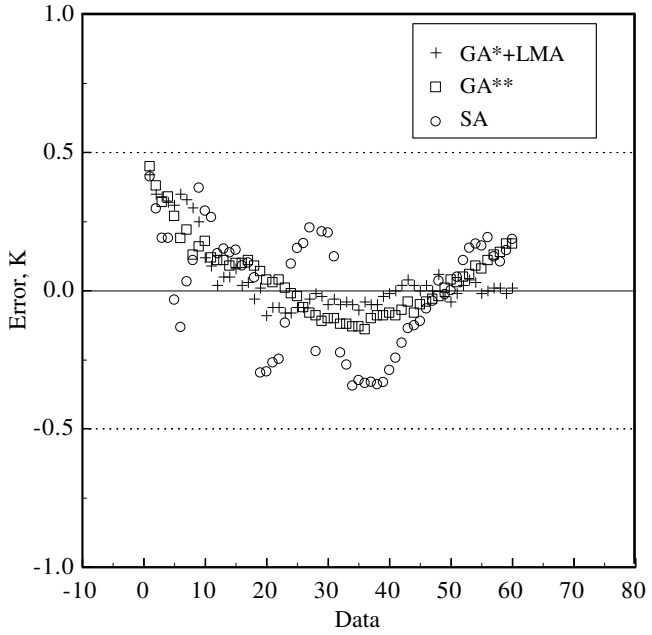

Fig. 5. Error between measured and simulated temperatures (corresponding to Expt. No.1). *GA output after 100 generations; **GA output after 300 generations.

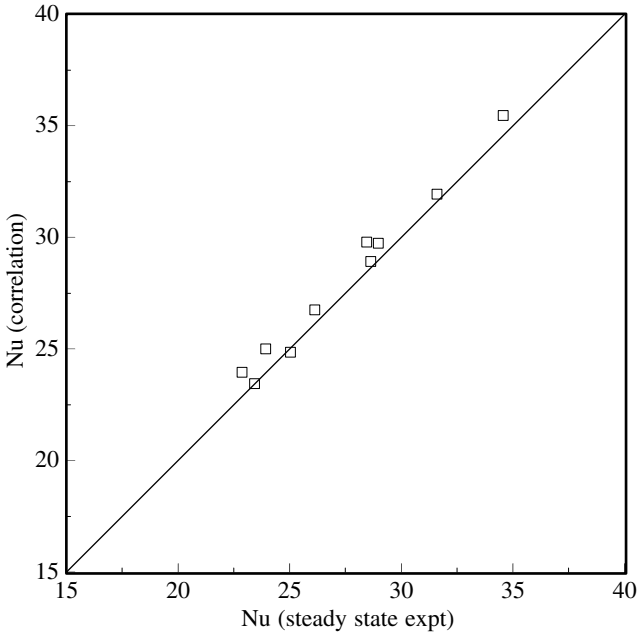

Fig. 7. Comparison of Nusselt number computed using the correlation with steady state results.

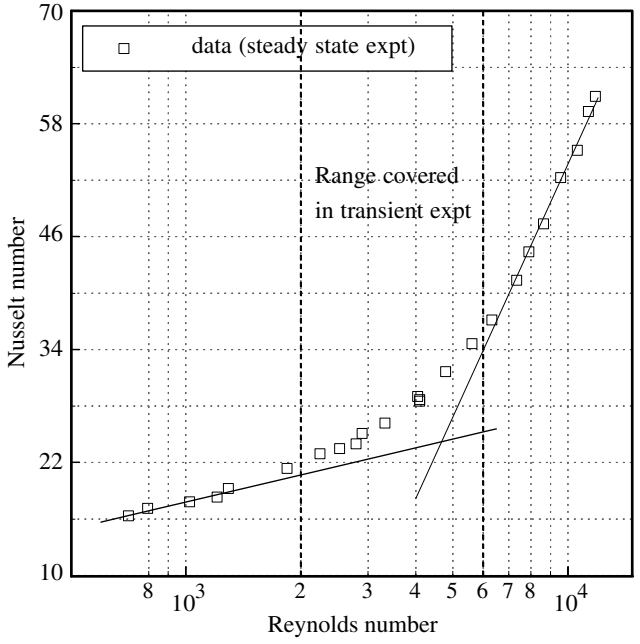

Fig. 6. Variation of Nusselt number with the channel Reynolds number.

parison shows that the Nusselt number values estimated using both the approaches are in good agreement. The validation exercise confirms the authenticity of the proposed approach for developing a heat transfer correlation, for a class of problems considered here, using a judicious combination of transient experimental techniques with a hybrid optimization method.

5. Uncertainty analysis

The uncertainties in the measured primary physical quantities are obtained from the calibration of the instruments or the uncertainty prescribed by the manufacturer. The propagation of error due to the uncertainties in the measured primary physical quantities into the estimation of Nusselt number is calculated using the procedure described in [29]. Following this procedure, the uncertainty in the estimation of radiosity is 1.25%, radiative heat transfer is 8.53%, convective heat transfer is 1.82%, convective heat transfer coefficient is 3.10% and the resulting uncertainty in the convective Nusselt number is estimated as 3.81%.

6. Conclusions

The expediency of transient cooling experiments combined with a hybrid optimization technique is explored to evolve a heat transfer correlation for low Reynolds number turbulent flows in vertical parallel plate channels. The novelty of the transient cooling experimental technique is that very few experimental runs are required to predict the coefficients and the exponents in a functional relation between dependent and independent variables. The highlight of the proposed transient experimental technique is that the concept of instantaneous Richardson number works well for a system having low thermal inertia for which quasi thermal equilibration is almost established. The hybridization of a stochastic optimization method with a gradient based method guarantees quick convergence to the optimum values of the parameters. The parameters were also retrieved using another global optimization technique namely Simulated Annealing and a good comparison of Nusselt number values of steady state experimental results with those estimated using the proposed correlation from the transient experimental technique reinforce the consistency of this approach.

References

[1] W. Elenbaas, Heat dissipation of parallel plates by free convection, Physica IX (1) (1942) 1–27.
[2] B. Gebhart, Y. Jaluria, R.L. Mahajan, B. Smmakia, Buoyancy Induced Flows and Transport, Hemisphere publishing corporation, Washington, DC, 1988.
[3] L.N. Tao, On combined free and forced convection in channels, ASME J. Heat Transfer 82 (1960) 233–238.
[4] H.C. Agarwal, A variational method for combined free and forced convection in channels, Int. J. Heat Mass Transfer 5 (1962) 439–444.

[5] J. Quintiere, W.K. Mueller, An analysis of laminar free, forced convection between finite vertical parallel plates, ASME J. Heat Transfer 95 (1973) 53–59.
[6] L.S. Yao, Free and forced convection in the entry region of a heated vertical channel, Int. J. Heat Mass Transfer 26 (1983) 65–72.
[7] W. Aung, G. Worku, Developing flow and flow reversal in a vertical channel with asymmetric wall temperatures, ASME J. Heat Transfer 108 (1986) 299–304.
[8] W. Aung, L.S. Fletcher, V. Sernas, Mixed convection in ducts with asymmetric wall heat fluxes, ASME J. Heat Transfer 109 (1987) 947–951.
[9] T.T. Hamadah, R.A. Writz, Analysis of laminar fully developed mixed convection in a vertical channel with opposing buoyancy, ASME J. Heat Transfer 113 (1991) 507–510.
[10] J.C. Watson, N.K. Anand, L.S. Fletcher, Mixed convection heat transfer between a series of vertical plates with planar heat sources, ASME J. Heat Transfer 118 (1996) 984–990.
[11] C. Gururaja Rao, C. Balaji, S.P. Venkateshan, Effect of surface radiation on conjugate mixed convection in a vertical channel with a discrete heat source in each wall, Int. J. Heat Mass Transfer 45 (2002) 3331–3347.
[12] M. Nakajima, K. Fukui, H. Ueda, T. Mizushina, Buoyancy effects on turbulent transport in combined free and forced convection between vertical parallel plates, Int. J. Heat Mass Transfer 23 (1980) 1325–1336.
[13] C.K. Chen, C.P. Chiu, S.C. Lee, Turbulent mixed flow of free and forced convection between vertical parallel plates, J. Thermophys. Heat Transfer 3 (1989) 454–460.
[14] G. Venugopal, C. Balaji, S.P. Venkateshan, A correlation for laminar mixed convection from vertical plates using transient experiments, Heat Mass Transfer 44 (2008) 1417–1425.
[15] R.W. Fox, A.T. McDonald, Introduction to Fluid Mechanics, 5th ed., John Wiley and sons, New York, 2001.
[16] G. Venugopal, M. Deiveegan, C. Balaji, S.P. Venkateshan, Simultaneous retrieval of total hemispherical emissivity and specific heat from transient multimode heat transfer experiments, ASME J. Heat Transfer 130 (2008) 061601-1–061601-8.
[17] F.P. Incropera, D.P. Dewitt, Fundamentals of Heat and Mass Transfer, 5th ed., John Wiley and sons, New York, 2002.
[18] A. Massa, D. Franceschini, G. Franceschini, M. Pastorino, M. Raffetto, M. Donelli, Parallel GA based approach for microwave imaging applications, IEEE Trans. Antennas Propagations 53 (2005) 3118–3127.
[19] J. Holland, Adaptation in Natural and Artificial Systems, MIT Press, Cambridge, MA, 1975.
[20] D.E. Goldberg, Genetic Algorithms in Search Optimization and Machine Learning, Addison-Wesley, New York, 1989.
[21] M. Deiveegan, C. Balaji, S.P. Venkateshan, Comparison of various methods for simultaneous retrieval of surface emissivities and gas properties in gray participating media, ASME J. Heat Transfer. 128 (2006) 829–837.
[22] V. Swaminathan, R.M. Gairola, C. Balaji, V.K. Agarwal, S.P. Venkateshan, Inverse radiation problem to retrieve hydrometeors from satellite microwave radiances, Int. J. Heat Mass Transfer 51 (2008) 1933–1945.
[23] D.W. Marquardt, An algorithm for least-squares estimation of nonlinear parameters, J. Soc. Indust. Appl. Math. 11 (1963) 431–441.
[24] B. Sawaf, M.N. Ozisik, Y. Jarny, An inverse analysis to estimate linearly temperature dependent thermal conductivity components and heat capacity of an orthotropic medium, Int. J. Heat Mass Transfer 38 (1995) 3005–3010.
[25] D.L. Carroll, Algorithms and optimizing chemical oxygen–iodine lasers, developments in theoretical and applied mechanics, in: H.B. Wilson, R.C. Batra, C.W. Bert, A.M. Davis, R.A. Schapery, D.S. Stewart, F.F. Swinson (Eds.), School of Engineering, vol. 18, The University of Alabama, 1996, pp. 411–424.
[26] C. Gau, K.A. Yih, Win Aung, Measurements of heat transfer and flow structure in heated vertical channels, J. Thermophys. Heat Transfer 6 (1992) 707–712.
[27] K. Deb, Optimization for Engineering Design: Algorithms and Examples, Prentice Hall of India, New Delhi, 2002.
[28] R.G. Eckert, R.J. Goldstein, Measurements in Heat Transfer, 2nd ed., Hemisphere Publishing Corporation, Washington, 1976.
[29] J.P. Holman, Experimental Methods for Engineers, 2nd ed., Mc Graw Hill, New York, 2001.